ISSN: 3064-9846
Research Article

Journal of Agricultural, Earth and Environmental Sciences

Channel Flow Field Recognition Method and Application Based on Eagle-eye Bionic Vision

Hairong Gao, Zihan Liu, & Yu Han*

College of Water Resources and Civil Engineering, China Agricultural University, Beijing 100083, China

***Corresponding author:** Yu Han, College of Water Resources and Civil Engineering, China Agricultural University, Beijing 100083, China.

Submitted: 11 September 2024 **Accepted:** 16 September 2024 **Published:** 24 September 2024

https://doi.org/10.63620/MKJAEES.2024.1052

Citation: *Gao, H., Liu, Z., & Han, Y. (2024). Channel flow field recognition method and application based on eagle-eye bionic vision. J of Agri Earth & Environmental Sciences 3(5), 01-08.*

Abstract

The monitoring of channel flow is a crucial aspect of quantitative water resource management. Based on the analysis of the hydrodynamic mechanism of ecological river channels, this manuscript establishes a cloud-edge integrated platform for the intelligent perception of hydrological information. It constructs an eagle-eye bionic vision intelligent flow measurement model and equipment suitable for multi-level canal networks, achieving real-time perception of water information and quantified representation of the entire flow field. The eagle-eye bionic vision intelligent flow measurement equipment integrates a monocular camera and a binocular camera. The monocular camera is utilized to capture surface flow images of the channel. Global surface flow velocity is inferred through dense optical flow analysis based on these images. The binocular camera recognizes the waterline based on the deep learning algorithm, constructs the triangular model of water level, measures point and distance measurement, senses the parallax depth in a binocular stereo sense, and monitors the water level information of the canal system in real time. Through binocular stereo vision, it perceives the disparity depth, enabling real-time monitoring of water level information in the channel system. Further integration of monocular flow measurement and binocular water depth recognition technologies, combined with logarithmic laws, allows for the derivation of cross-sectional average flow velocity. The constructed eagle-eye bionic visual intelligent flow measurement equipment technology can promote the deep integration of water conservancy business and information technology, provide a reference for optimizing water resource allocation in irrigation areas, and promote the automation, intelligence, and high-quality development of water measurement equipment.

Keywords: Eagle-Eye Bionic Vision, Channel Flow Field Identification, Intelligent flow Measurement Equipment.

Introduction

Irrigation is one of the principal factors enhancing crop yield, with irrigation districts constituting vital public infrastructure projects in China, crucial for national food security. Moreover, the most substantial water-saving potential lies within these irrigation districts. Monitoring water flow serves the primary purpose of understanding the state of water resources, encompassing parameters such as flow rate, velocity, and water level, facilitating improved planning, management, and conservation of water resources [1-6]. With the influence of machine vision on the development of water conservancy information construction, video monitoring is also more and more used in irrigation area monitoring, and researchers at home and abroad have conducted in-depth research on this [7-11]. Liu et al. proposed a method for measuring flow velocity in mountainous streams in Northern China, simulating the actual water surface using geometric coordinates from images, and fitting the positions of floating markers captured by cameras into image coordinates to compute flow velocity [12]. Lee MC et al. introduced and applied an improved method for determining the depth and flow rate of river sections using X-band radar technology, successfully tracking floating objects on the river surface and measuring flow velocity [13]. J.D.Cretin et al. employed foam generated on the river surface as a target, measuring flow velocity through video

monitoring of floating objects [14]. However, this method has limitations; shadows caused by water surface refraction hinder the accurate identification of tracing particles or water surface ripples, posing challenges to flow velocity calculation. Bradley et al. used branches floating on the river surface as tracers to calculate flow velocity [15]. Velocity measurement data were employed as inputs for a hydraulic model, deriving a three-dimensional flow field based on kinematic principles. However, the absence of cross-sectional measurements during velocity measurement may lead to certain errors. Fujita et al. applied the PIV algorithm to measure actual river flow velocity using image processing technology, proposing the LS-PIV technique suitable for large-scale image particle velocimetry [16]. They estimated river flow velocity by applying large-scale particle image technology to a small river within a 300-meter range, presenting practical applications of the LS-PIV system in small rivers and providing corresponding suggestions and conclusions. Kang et al. achieved target recognition and distance measurement using a visual system, enhancing computational speed by acquiring disparity removing residual parts of images outside the identified objects [17].

Based on this, this study proposed the eagle-eye bionic vision intelligent flow measurement equipment and technology for high-precision flow measurement in irrigation areas. Utilizing monocular cameras, the dense optical flow method is employed to obtain global surface flow velocity, while binocular cameras are used to acquire channel water level information. Finally, by utilizing the obtained values of surface flow velocity and water level, the eagle-eye vision intelligent flow measurement equipment is constructed, enabling fully automated flow measurement in channels. This contribution provides theoretical and technical support for the construction of digital twin irrigation district systems, holding significant practical implications.

Methods

Experimental Site

In July 2023, the eagle-eye bionic vision intelligent flow measurement equipment test was carried out in the Xiwu Canal of Jin 'an Irrigation District in Xinjiang. The length of the test section of the Xiwu Canal is about 80 m and the width is about 4.2 m. During the experiment, the monocular camera and binocular camera were taken in video mode, and the image resolution was 3840 × 2160 pixels. The shooting time is about 10 minutes once, 100 s video is selected, 1200 frames are extracted for analysis, and the interval between adjacent images is 0.4 s. The measured value of the water level is recorded by the level meter combined with the tower ruler to verify the accuracy of the machine vision to identify the water level. The portable flow meter is used to measure and record the flow velocity of the channel, and the accuracy of the dense optical flow method is verified.

Figure 1: Equipment demonstration of Jin 'an irrigation area in Xinjiang

Eagle-eye Bionic Vision

At the same time, the human eye can only focus on a small portion of the field of view. Eagles, however, are able to rapidly locate multiple targets even under divided attention, utilizing their visual advantages to lock onto targets at far distances and estimate distances for hunting purposes. Based on this, by simulating the characteristics of eagle-eye cone cells that recognize texture brightness at ultra-long distances, we construct an eagle-eye bionic vision model. On one hand, we utilize depth vision to locate and perceive the distance of canal shorelines, reconstructing the target scene for identifying canal water levels. On the other hand, by discretizing the vector features of water ripples and waves, we accurately perceive surface flow velocities in the canal.

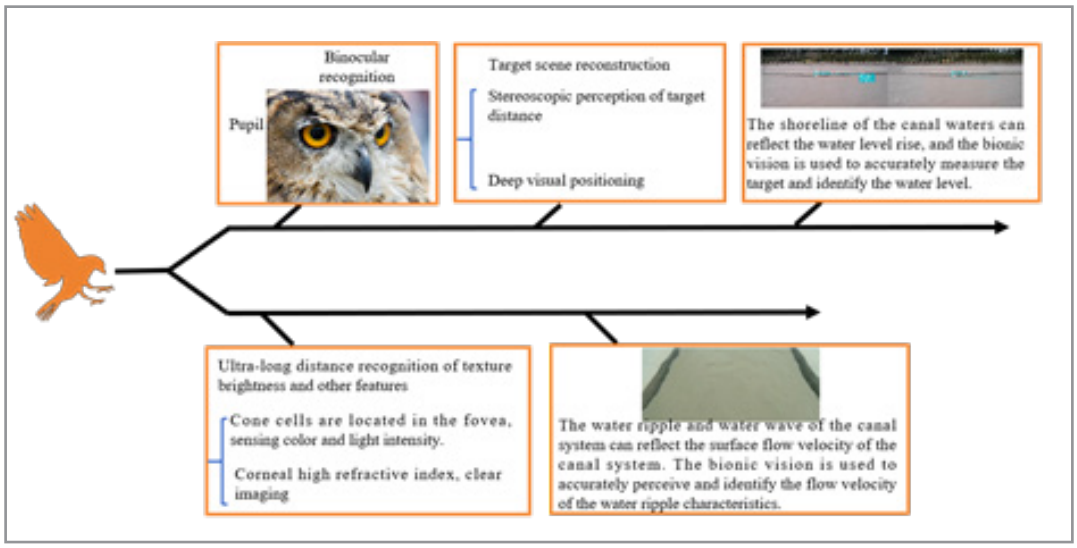

Figure 2: Functionalities of Eagle-eye Bionic Vision

Water Level Calculation Method

The video data obtained from the binocular cameras was processed using the frame differencing method to convert it into image data. The YOLOv8 model for target water level identification was employed, utilizing a dataset derived from the experimental video recordings. The dataset comprised 80% of the data for training, 10% for validation, and 10% for testing, with a final selection of 500 images for training data. Data augmentation techniques were applied, and the dataset was annotated using Labellmg software to mark the boundaries of the canal and record the positions and relevant coordinate information of the labels. Subsequently, the algorithm was trained. The training and validation of the shoreline image dataset were performed, aiming to achieve higher accuracy in shoreline delineation by increasing the number of model training iterations. Based on the Principle of Corresponding Points in PCN, the distance (c) between the binocular cameras and the shoreline was obtained. According to the cosine theorem, the vertical distance (a) from the binocular cameras to the shoreline was calculated as $a=c\times\cos\alpha$, where the canal cross-section water level value (h) was determined as $h=m-a$.

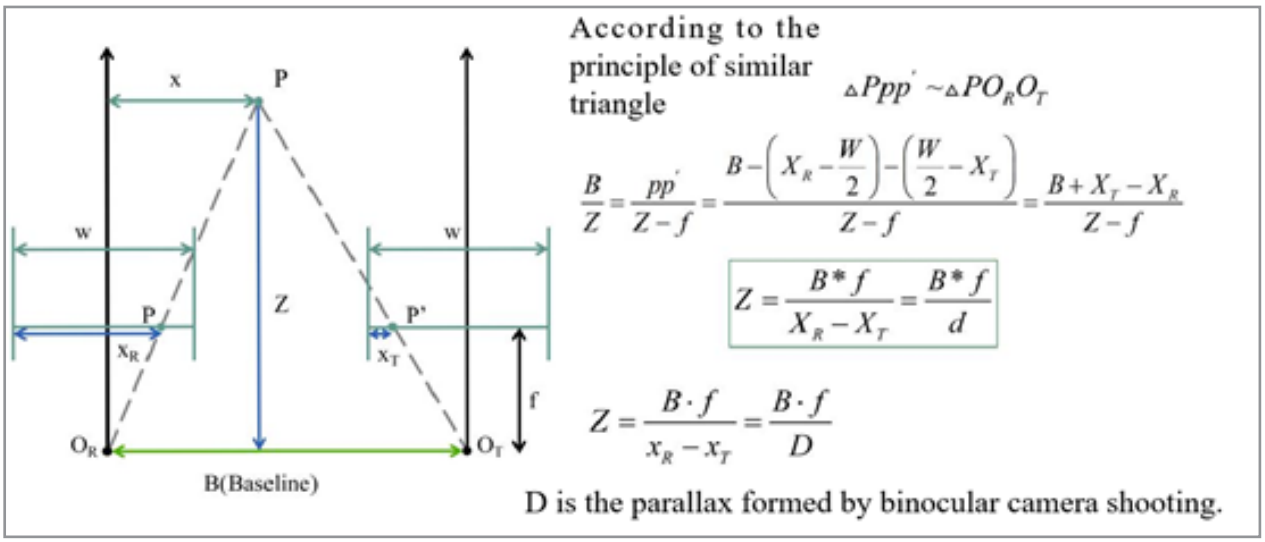

Figure 3: Principle Diagram of PCN Ranging

Flow Velocity Calculation Method

The definition of the optical flow method for detecting target motion is to search for pixels in corresponding positions of adjacent or alternate frames with high correlation in pixel threshold, recording the vector direction and pixel displacement of the target object between each frame. Its basic idea is to assign a velocity vector to each pixel point in the image, thus forming the motion field of the image. Points on the image and points on a three-dimensional object are one-to-one correspondence at a specific moment of motion, and the image is dynamical-

ly analyzed based on the velocity vector characteristics of each pixel point. If there are no moving targets in the image, the optical flow vector in the entire image area will be continuously changing. However, when there is relative motion between the object and the image background, the velocity vector formed by the moving object will inevitably be different from the velocity vector of the neighborhood background, thus detecting the position of the moving object. In this study, the dense optical flow method was adopted. This algorithm assumes that the gradient of the image is constant, and the local optical flow is constant. The expression of constant local optical flow is:

$$d = \frac{\partial X}{\partial t} \quad (1)$$

This algorithm estimates displacement through polynomial variations. Based on the assumption of optical flow method, displacement d can be calculated:

$$\mathrm{d} = \frac{-A_1^{-1}(b_2 - b_1)}{2} \quad (2)$$

In the equation, A1, b1, and b2 are coefficients of quadratic polynomial matrix functions.

Calculation of Mean Flow Velocity for Cross-section

To achieve precise irrigation in open channels within irrigation districts and ensure the rational allocation of water resources, it is essential to accurately understand the velocity distribution of water flow in open channels. This facilitates convenient and straightforward deployment of measurement points and further calculation of water flow in open channels. Since the introduction of the boundary layer concept by Prandtl in 1904, boundary layer theory has been applied by researchers in hydraulic studies, opening up new perspectives for understanding fluid motion in practical boundary conditions and advancing the field of hydraulics. It was not until 1938 that Keulegen proposed the use of the logarithmic formula to describe the velocity distribution of uniform turbulent flow in open channels. Therefore, the logarithmic formula has since been employed in the study of velocity distribution in uniform turbulent flow in open channels. In this study, the logarithmic law is used for calculating the mean flow velocity across sections, with the calculation formula as follows:

$$\mathrm{u} = A \ln y + B \quad (3)$$

Where, A represents , B represents $u = A\ln\left(\frac{u_*}{v}\right) + Bu_*$, B represents the correlation coefficient, u* represents the local shear velocity, v represents the kinematic viscosity of water, y represents the distance from each point on the vertical line in the channel to the sidewall.

Results and Discussion

Analysis of Water Level Recognition Results Based on Eagle-eye Bionic Vision

The experiment utilized binocular captured video streams for testing. Specifically, a segment of the video was selected from both the training and validation sets for simulated recognition. The duration of the training set was 52 seconds, with no misidentification observed, while the duration of the validation set was 47 seconds, with 1 second of misidentification. Figure 4 illustrates the evaluation results of the YOLO model for shoreline identification in each iteration. After 300 iterations, the model reached a convergent state. Throughout the training process, both the precision and recall of the model remained stable. Once the model reached saturation, its precision could consistently maintain above 95%, and the recall rate could remain stable at around 100%. The average precision and mean Average Precision (mAP) also remained at a high level, approximately 1.0. The sum of mean Average Precision values stayed above 0.9. These results indicate that the YOLO model achieved good accuracy in shoreline identification on the training set. With a recognition accuracy of 100% on the training set videos, it suggests that the features of the dataset were fully recognized during the training process, and after 300 rounds of training, the model's recognition accuracy reached its peak. The recognition accuracy for the validation set was 95.6%, indicating that the model achieved a recognition accuracy of 95.6% for the features under study.

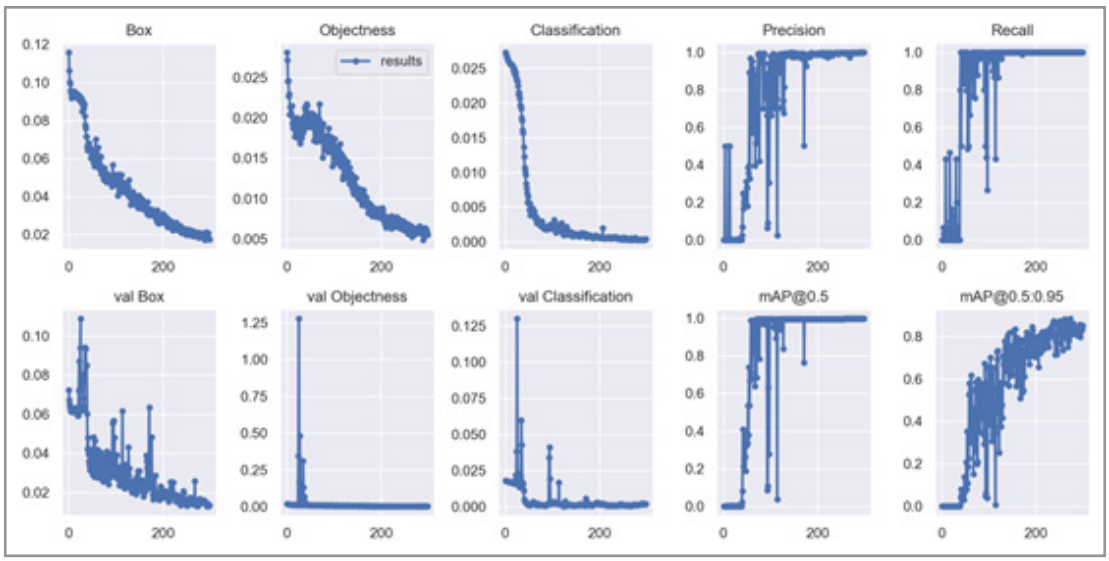

Figure 4: Evaluation of Shoreline Accuracy on Training Set

Applying eagle-eye bionic vision for channel water level recognition, a comparison was made between the measured water depth and the water depth values obtained using the PCN algorithm to validate the accuracy of the PCN algorithm. By setting deviation angles of 40~80° and camera-to-ground distances of 50-100cm, the conditions were compared. From Figure 5, it can be observed that the model's accuracy exceeds 93%. The lower the distance between the camera and the ground, the higher the accuracy of water level recognition, and the better the fitting results. Moreover, under the condition of a 40° deviation angle of the camera, the error between the calculated water level and the measured value is minimized, at 2%. Additionally, the residual between the water level calculated using eagle-eye bionic vision and the measured value is within ±0.02, indicating that the standard error between the measured value and the calculated value follows a normal distribution. This implies that the model used is reasonable, indicating a good water level recognition effect.

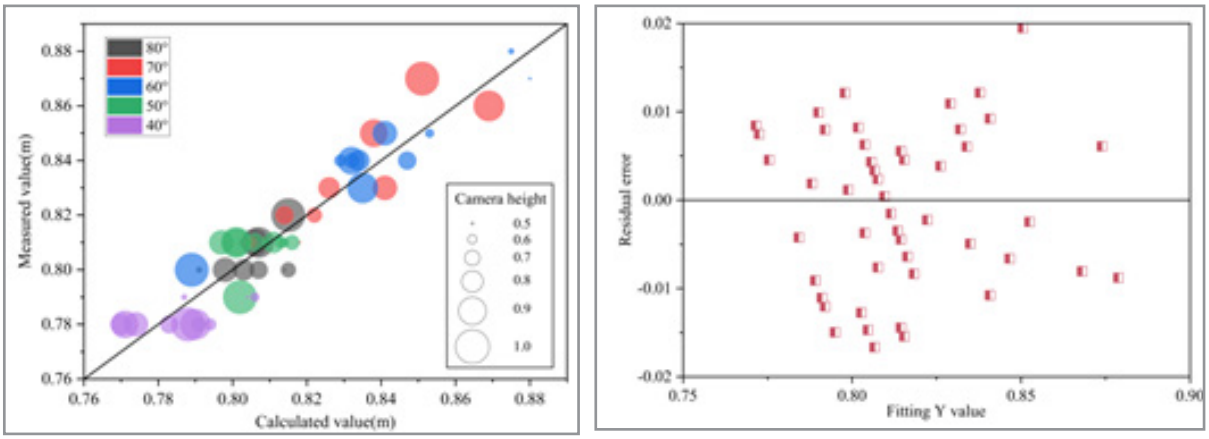

Figure 5: Results of Canal Water Level Recognition and Residuals Using Eagle-eye Bionic Vision

Analysis of Flow Velocity Calculation Results Based on Eagle-eye Bionic Vision

Applying the Dense Optical Flow model for the recognition of surface flow velocity in the channel, water ripple, and wave video streams were obtained frame by frame. Using the principle of monocular ranging, pixel coordinates were converted into actual coordinates, obtaining the actual distance the water moved over a certain period. This actual distance was divided by the corresponding time to calculate the surface flow velocity in the channel. Additionally, an impeller flowmeter was utilized to calculate the actual velocity of the water flow. The calculated velocities were compared and analyzed against the actual velocities. Figure 6 compares the surface flow velocities at different periods. It can be observed from the figure that the four surface flow velocities are roughly symmetrically distributed, with the maximum velocity located in the middle of the channel. Due to perennial water flow in the channel, sedimentation of silt occurs at the bottom of the channel, leading to fluctuations in the maximum flow velocity in the middle of the channel. The calculated values of flow velocity using the optical flow method and the measured values exhibit consistent trends in flow distribution. A comparison between the measured and calculated values of the four surface flow velocities reveals that, overall, the velocities obtained by the optical flow method are slightly larger than the measured values. The fitting effect is good under low flow rate and low flow velocity conditions, with errors within 10% for flow rates between 2.9~3.5 m^3/s. However, at a flow rate of 3.5 m^3/s, the error is relatively larger, within 15%. This indicates that the channel flow distribution model can accurately describe the global real flow velocity distribution. Furthermore, Figure 7 shows a good fitting effect between the measured and calculated values, with a model accuracy of over 95%.

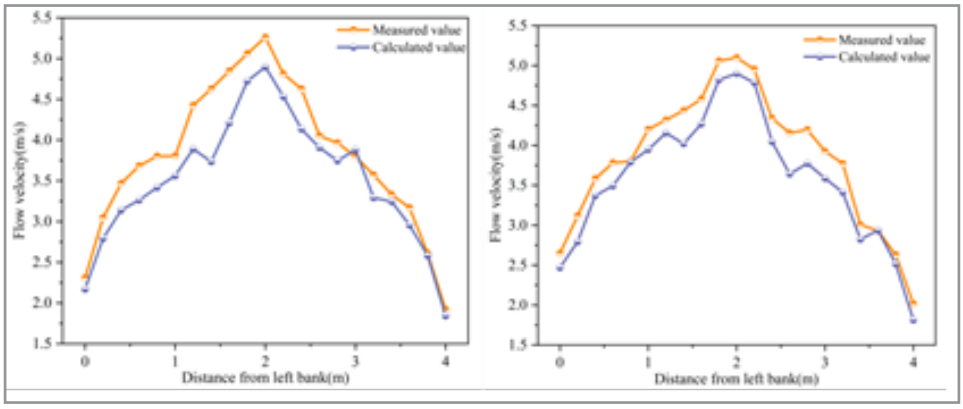

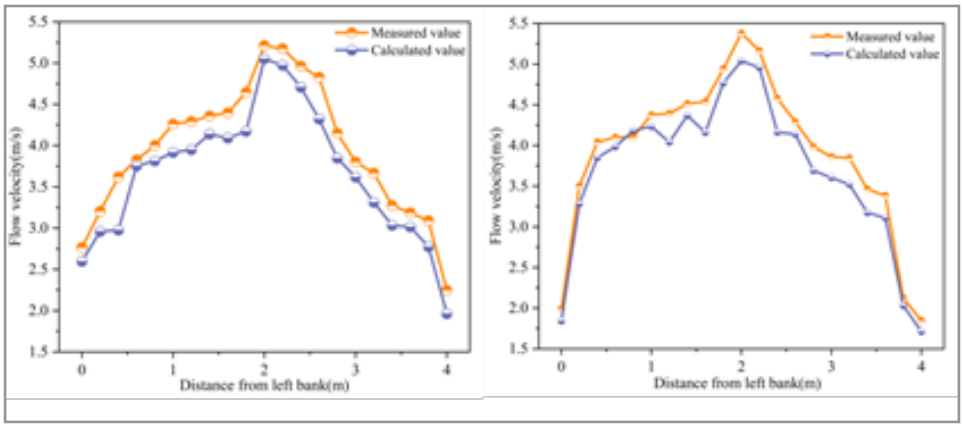

Figure 6: Distribution of Optical Flow Velocity and Measured Velocity

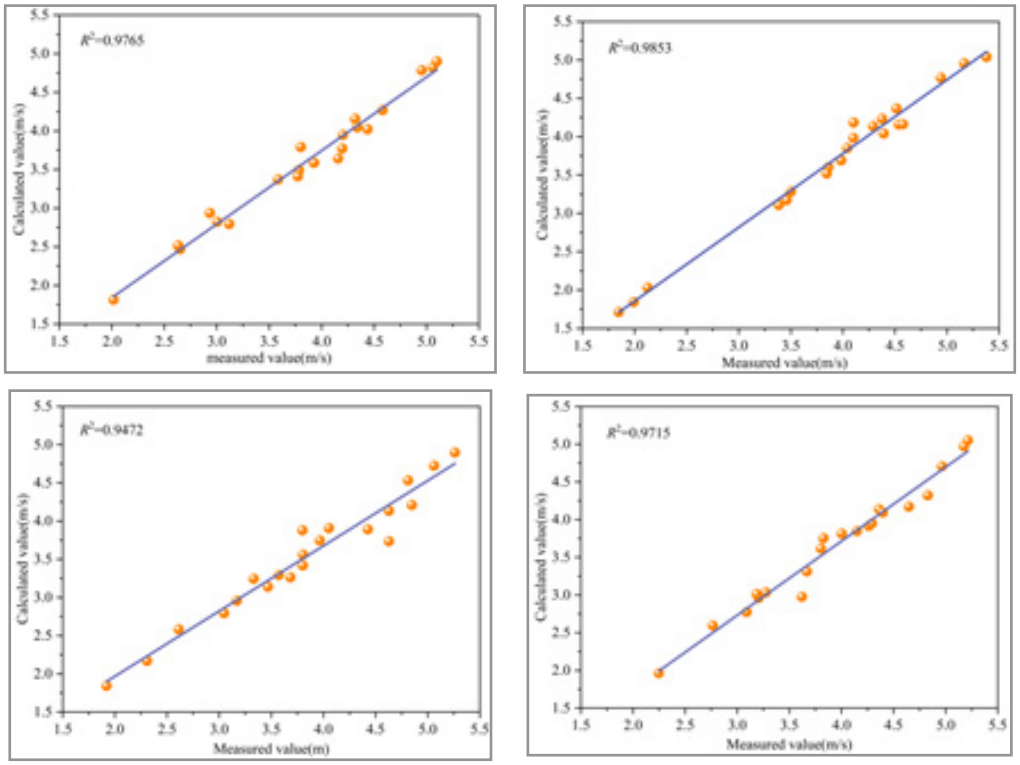

Figure 7: Comparison of Accuracy Between Measured and Calculated Flow Velocities

Analysis of Results for Mean Flow Velocity Calculation Across Sections

To calculate the flow rate across the channel section, it is necessary to obtain the velocity distribution across the entire section. This involves integrating the water level values calculated using the YOLO algorithm based on deep learning and the surface flow velocities calculated using the dense optical flow method. Once the values of A and B in the formula for calculating the velocity distribution across the section are determined, the velocity across the entire section can be calculated using these values. As shown in Figure 8, the distribution of velocity across the section can be obtained by analyzing the velocity distribution pattern across different zones of the section. The velocity distribution across the entire section of the channel exhibits a roughly symmetrical pattern. Analyzing the flow velocity in the normal direction, it is observed that the velocity increases when moving away from the sidewalls, with the maximum velocity occurring at the water surface. This is because the sidewall resistance is high, resulting in a lower velocity along the sidewalls of the channel section.

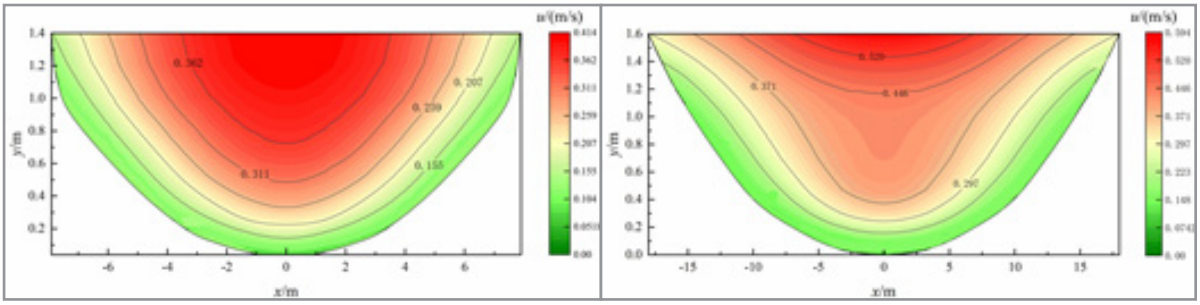

Figure 8: Distribution of Flow Velocity Across Channel Section

Conclusion

In the context of smart water management, automated flow measurement is particularly important, with flow velocity measurement being a key parameter for flow rate calculation. Achieving automated flow measurement holds significant significance for water resource management and water pricing formulation. Manual measurement of flow velocity requires a considerable amount of manpower, and field conditions are often harsh, making data recording and transmission difficult and unable to meet the requirements of intelligent flow measurement [18-20]. Therefore, this paper proposes a method for channel flow field recognition based on eagle-eye bionic vision. Machine vision for measuring water flow velocity is achieved using the dense optical flow method. The YOLO algorithm is a method based on convolutional neural networks for tracking images. This paper combines YOLO with PCN for water level recognition, further integrates monocular flow measurement and binocular water level recognition technology and utilizes the logarithmic law to calculate the mean flow velocity across sections.

1. The application of the optical flow method and YOLO algorithm to channel flow field recognition indicates that the calculated flow velocity and water level values are close to the actual flow velocity measured by the portable flowmeter and the water level values measured by the staff gauge, with a model accuracy of over 90%.
2. The combination of monocular flow measurement and binocular water level recognition technology, along with the logarithmic law, allows for the accurate calculation of mean flow velocity across sections.

References

1. Zhiyu, L., Yuhuan, L., & Xiangyi, K. (2021). Problems, strategies and key technology research of flood forecasting and early warning for small and medium-sized rivers. Journal of Hohai University (Natural Sciences), 49, 1-6.
2. Fu, M., Luo, Z., Feng, L., & Que, X. (2023). Water productivity maximization and ecosystem monitoring to estimate tourism economic value. Water Supply, 23, 4672-4681.
3. Letessier, C., Cardi, J., Dussel, A., Ebtehaj, I., & Bonakdari, H. (2023). Enhancing flood prediction accuracy through integration of meteorological parameters in river flow observations: A case study of Ottawa River. Hydrology, 10, 164.
4. Maranzoni, A., D'Oria, M., & Rizzo, C. (2023). Quantitative flood hazard assessment methods: A review. Journal of Flood Risk Management, 16, e12855.
5. Ichiro, F. (2017). Discharge measurements of snowmelt flood by space-time image velocimetry during the night using far-infrared camera. Water, 9, 269.
6. Lin, Y. C., Ho, H. C., Lee, T. A., & Chen, H. Y. (2022). Application of image technique to obtain surface velocity and bed elevation in open-channel flow. Water, 14, 1895.
7. Zhu, Y., Zhang, Y., Yang, J., Nguyen, B. T., & Wang, Y. (2022). A novel method for calculating distributed water depth and flow velocity of stormwater runoff during the heavy rainfall events. Journal of Hydrology, 612, 128064.
8. Zhao, H., Chen, H., Liu, B., Liu, W., & Xu, C. Y. (2020). An improvement of the Space-Time Image Velocimetry combined with a new denoising method for estimating river discharge. Flow Measurement and Instrumentation, 77, 101864.
9. Zhen, Z., Huabao, L., Yang, Z., & Jian, H. (2019). Design and evaluation of an FFT-based space-time image velocimetry (STIV) for time-averaged velocity measurement. In 2019 14th IEEE International Conference on Electronic Measurement & Instruments (ICEMI) (pp. 503-514). IEEE.
10. Tsubaki, R. (2017). On the texture angle detection used in space-time image velocimetry (STIV). Water Resources Research, 53, 10908-10914.
11. Liu, C., Wen, B., Duan, Z., & Tian, Y. (2022). Measurement of mountain river discharge based on UHF radar. IEEE Geoscience and Remote Sensing Letters, 20, 1-5.
12. Liu, J., He, Z., & Li, B. (2003). Introduction to the method of surface flow velocity measurement using image techniques. Hydrology, 53, 54-61.
13. Lee, M. C., Leu, J. M., Lai, C. J., Plant, W. J., & Keller, W. C. (2002). Non-contact flood discharge measurements using an X-band pulse radar (II) Improvements and applications. Flow Measurement and Instrumentation, 13, 271-276.
14. Creutin, J. D., Muste, M., Bradley, A. A., Kim, S. C., & Kruger, A. (2003). River gauging using PIV techniques: A proof of concept experiment on the Iowa River. Journal of Hydrology, 277, 182-194.
15. Bradley, A. A., Kruger, A., Meselhe, E. A., & Muste, M. (2002). Flow measurement in streams using video imagery. Water Resources Research, 38, 8.
16. Fujita, I., Muste, M., & Kruger, A. (1998). Large-scale particle image velocimetry for flow analysis in hydraulic engineering applications. Journal of Hydraulic Research, 36, 397-414.
17. Kang, H. S., Lee, N. H., & Lee, J. M. (2018). Distance measurement algorithm based on object recognition. In Interna-

tional Conference on Artificial Life and Robotics (ICAROB) 2018 (pp. 290-293).
18. Dolcetti, G., Hortobágyi, B., Perks, M., Tait, S. J., & Dervilis, N. (2022). Using non-contact measurement of water surface dynamics to estimate river discharge. Water Resources Research, 58, e2022WR032829.
19. Maceas, M., Osorio, A. F., & Bolanos, F. (2021). A methodology for improving both performance and measurement errors in PIV. Flow Measurement and Instrumentation, 77, 101846.
20. Muste, M., Fujita, I., & Hauet, A. (2008). Large-scale particle image velocimetry for measurements in riverine environments. Water Resources Research, 44, W00D19.